

Gravitational lensing by Charged black hole in regularized 4D Einstein-Gauss-Bonnet gravity

Rahul Kumar,^{1,*} Shafqat Ul Islam,^{1,†} and Sushant G. Ghosh^{1,2,‡}

¹*Centre for Theoretical Physics, Jamia Millia Islamia, New Delhi 110025, India*

²*Astrophysics and Cosmology Research Unit, School of Mathematics, Statistics and Computer Science, University of KwaZulu-Natal, Private Bag 54001, Durban 4000, South Africa*

(Dated: April 28, 2020)

Among the higher curvature gravities, the most extensively studied theory is the so-called Einstein-Gauss-Bonnet (EGB) gravity, whose Lagrangian contains Einstein term with the GB combination of quadratic curvature terms, and the GB term yields nontrivial gravitational dynamics in $D \geq 5$. Recently there has been a surge of interest in regularizing, a $D \rightarrow 4$ limit, the EGB gravity, and the resulting regularized 4D EGB gravity has nontrivial dynamics. We consider gravitational lensing by Charged black holes in the regularized 4D EGB gravity theory to calculate the deflection coefficients \bar{a} and \bar{b} , while former increases with increasing GB parameter α and charge q , later decrease. We also find a decrease in the deflection angle α_D , angular position θ_∞ decreases more slowly and impact parameter for photon orbits u_m more quickly, but angular separation s increases more rapidly with α and charge q . We compare our results with those analogous black holes in General Relativity (GR) and also formalism is applied to discuss the astrophysical consequences in the case of the supermassive black holes Sgr A*.

I. INTRODUCTION

General Relativity (GR) not only predicts the existence of black holes but also a mean to observe them through the gravitational impact on the electromagnetic radiation moving in the near vicinity of black holes. The advent of horizon-scale observations of astrophysical black holes [1, 2] offer an unprecedented opportunity to understand the intricate details of photon geodesics in the black hole spacetimes [3, 4], which has become of physical relevance in present-day astronomy. Photons passing in the gravitational field of a compact astrophysical object get deviate from their original path and the phenomenon is known as the gravitational lensing [5–7]. Though the theory of gravitational lensing was primarily developed in the weak-field thin-lens approximation for small deflection angles [8, 9], but in black hole spacetimes, where photons can traveled close to the gravitational radius, a full treatment of lensing theory valid even in strong-field gravity regime is required. Darwin [7] led the study of strong gravitational lensing theory, and later Virbhadra and Ellis [10] numerically calculated the deflection angle due to the Schwarzschild black hole in an asymptotically flat background. Using an alternative formulation, Frittelli, Kling and Newman [11] analytically obtained an exact lens equation. A significant interest in the strong gravitational lensing is developed by the Bozza et al. [12], who gave a general and systematic investigation of light bending in the strong-gravity region, and exploiting the source-lens-observer geometry obtained the analytical

expressions for the source's images positions.

One of the generic features of strong gravitational lensing is the logarithmic divergence of the deflection angle in the impact parameter and the existence of relativistic images, which are produced due to multiple winding of light around the black hole before emanating in observer's direction [13]. The strong gravitational lensing relevance for predicting the strong-field features of gravity, testing and comparing various theories of gravity in strong-field regime, estimating black hole parameters, and deducing any matter distributions in black hole background have resulted in a vast comprehensive literature [14–18]. Also, gravitational lensing from various modifications of Schwarzschild geometry arising due to modified gravities, e.g., regular black holes [19, 20], massive gravity black holes [21], $f(R)$ black holes [22] and also in Einstein-Gauss-Bonnet (EGB) gravity models [23].

EGB gravity theory is a natural extension of GR to higher dimensions $D \geq 5$, in which Lagrangian density admits quadratic corrections constructed from the curvature tensors invariants [24, 25]. The EGB gravity, which naturally appears in the low-energy limit of string theory [26], preserves the degrees of freedom and is free from gravitational instabilities and thereby leads to the ghost-free nontrivial gravitational self-interactions [27]. Due to much broader theoretical setup and consistency with the available astrophysical data, EGB gravity had been widely studied in varieties of context over the past decades [28–30].

The Gauss-Bonnet (GB) correction to the Einstein-Hilbert action is a topological invariant in $D = 4$ and therefore does not make any contribution to the gravitational dynamics. This issue has been addressed by Glavan and Lin [31] by re-scaling the GB coupling parameter as $\alpha \rightarrow \alpha/(D-4)$ and defining the 4D theory as the limit of $D \rightarrow 4$ at the level of field's equation. This

*Electronic address: rahul.phy3@gmail.com

†Electronic address: Shafphy@gmail.com

‡Electronic address: sgghosh2@jmi.ac.in, sgghosh@gmail.com

kind of regularization was earlier proposed by Tomozawa [32] as quantum corrections to Einstein gravity, and they also found the spherically symmetric black hole solution. Later Cognola *et al.* [33] gave a simplified approach for Tomozawa [32] formulation, which mimic quantum corrections due to a GB invariant within a classical Lagrangian. Further, the static and spherically symmetric black hole solution [31–33] of 4D EGB gravity is identical as those found in semi-classical Einstein's equations with conformal anomaly [34], regularized Lovelock gravity [35, 36], and the Horndeski scalar-tensor theory [37].

Hence, the 4D EGB gravity witnessed significant attentions that includes finding black hole solutions and investigating their properties [38–40], Vaidya-like solution [41], black holes coupled with magnetic charge [42], and also rotating black holes [43]. Other probes include gravitational lensing [44], black hole shadows, [43, 45, 46], derivation of regularized field equations [47], Morris-Thorne-like wormholes [48], and black hole thermodynamics [49]. Nonetheless, several questions [50–54] have been raised on the procedure adapted in [31, 33], and also some remedies have been suggested to overcome [35, 37, 51, 55]. However, it turns out the spherically symmetric 4D black hole solution found in [31, 33] remains valid for these regularized theories [35, 37, 51], but may not beyond spherical symmetry [51].

This motivated us to consider the gravitational lensing by Charged black hole in regularized 4D EGB gravity. Following the prescription of Bozza *et al.* [12], we determine the strong deflection coefficients and the resulting deflection angle, which becomes unboundedly large for smaller impact parameter values. Positions and magnifications of source's relativistic images are determined and the effect of charge is investigated. We also obtained the corrections in the deflection angle due to the GB coupling parameter in the supermassive black hole contexts.

The rest of paper is organized as follows. In the Sect. II, we discuss the static spherically symmetric Charged black hole in 4D EGB gravity. Formalism for gravitational bending of light in strong-field limit is setup in Sect. III, whereas strong-lensing observables, numerical estimations of deflection angle, and image positions and magnifications are presented in Sect. IV. Lensing by supermassive black hole Sgr A* is discussed in Sect. IV. Finally, we summarize our main findings in Sect. VI.

II. CHARGED BLACK HOLES IN 4D EGB GRAVITY

The EGB gravity action with re-scaled coupling constant $\alpha/(D-4)$ and minimally coupled electromagnetic field in D dimensional spacetime

reads [39]

$$S = \frac{1}{16\pi G} \int d^D x \sqrt{-g} [R + \frac{\alpha}{D-4} \mathcal{G} - F_{\mu\nu} F^{\mu\nu}], \quad (1)$$

with \mathcal{G} is the GB term defined by

$$\mathcal{G} = R^2 - 4R_{\mu\nu}R^{\mu\nu} + R_{\mu\nu\rho\sigma}R^{\mu\nu\rho\sigma}, \quad (2)$$

g is the determinant of metric tensor $g_{\mu\nu}$, R is the Ricci scalar, and $F_{\mu\nu} = \partial_\mu A_\nu - \partial_\nu A_\mu$ is the Maxwell tensor with A_μ being the gauge potential. On varying the action (1) with respect to the metric tensor $g_{\mu\nu}$, we obtain the field's equation

$$G_{\mu\nu} + \frac{\alpha}{D-4} H_{\mu\nu} = T_{\mu\nu} \equiv 2 \left(F_{\mu\sigma} F^\sigma{}_\nu - \frac{1}{4} g_{\mu\nu} F_{\alpha\beta} F^{\alpha\beta} \right), \quad (3)$$

where $G_{\mu\nu} = R_{\mu\nu} - \frac{1}{2} R g_{\mu\nu}$ is the Einstein's tensor, and $H_{\mu\nu}$ is the Lanczos tensor [24] and is given by

$$H_{\mu\nu} = 2(RR_{\mu\nu} - 2R_{\mu\sigma}R^\sigma{}_\nu - 2R_{\mu\sigma\nu\rho}R^{\sigma\rho} - R_{\mu\sigma\rho\beta}R^\sigma{}_\nu{}^{\rho\beta}) - \frac{1}{2} g_{\mu\nu} \mathcal{G}, \quad (4)$$

and $T_{\mu\nu}$ is the energy-momentum tensor for the electromagnetic field. Considering a static and spherically symmetric D -dimensional metric ansatz

$$ds^2 = -f(r)dt^2 + \frac{1}{f(r)}dr^2 + r^2 d\Omega_{D-2}^2, \quad (5)$$

and where $d\Omega_{D-2}$ is the metric of a $(D-2)$ -dimensional spherical surface. Solving the field equations (3), in the limit $D \rightarrow 4$, yields a solution [39]

$$f_{\pm}(r) = 1 + \frac{r^2}{2\alpha} \left(1 \pm \sqrt{1 + 4\alpha \left(\frac{2M}{r^3} - \frac{Q^2}{r^4} \right)} \right). \quad (6)$$

Here, M and Q can be identified, respectively, as the mass and charge parameters of the black hole. In the limit of $Q = 0$, metric (5) with (6) corresponds to the static 4D EGB black hole [31]. Equation (6) corresponds to the two branches of solutions depending on the choice of “ \pm ”, such that at large distances Eq. (6) reduces to

$$f_-(r) = 1 - \frac{2M}{r} + \frac{Q^2}{r^2}, \quad f_+(r) = 1 + \frac{2M}{r} - \frac{Q^2}{r^2} + \frac{r^2}{\alpha}. \quad (7)$$

In the vanishing limit of α only -ve branch smoothly recovers the Reissner-Nordstrom black hole [39]. Thus, we will limit our discussions to -ve branch only. The effect of GB coupling parameter faded at large distances, as the Charged black holes in 4D EGB gravity smoothly retrieve the Reissner-Nordstrom black hole. However, considerable departure can be expected in strong-field regime where usually full features of GB corrections come in to play. The Charged black holes in 4D EGB gravity are characterized uniquely by mass M , charge Q , and GB parameter α . To begin a discussion on

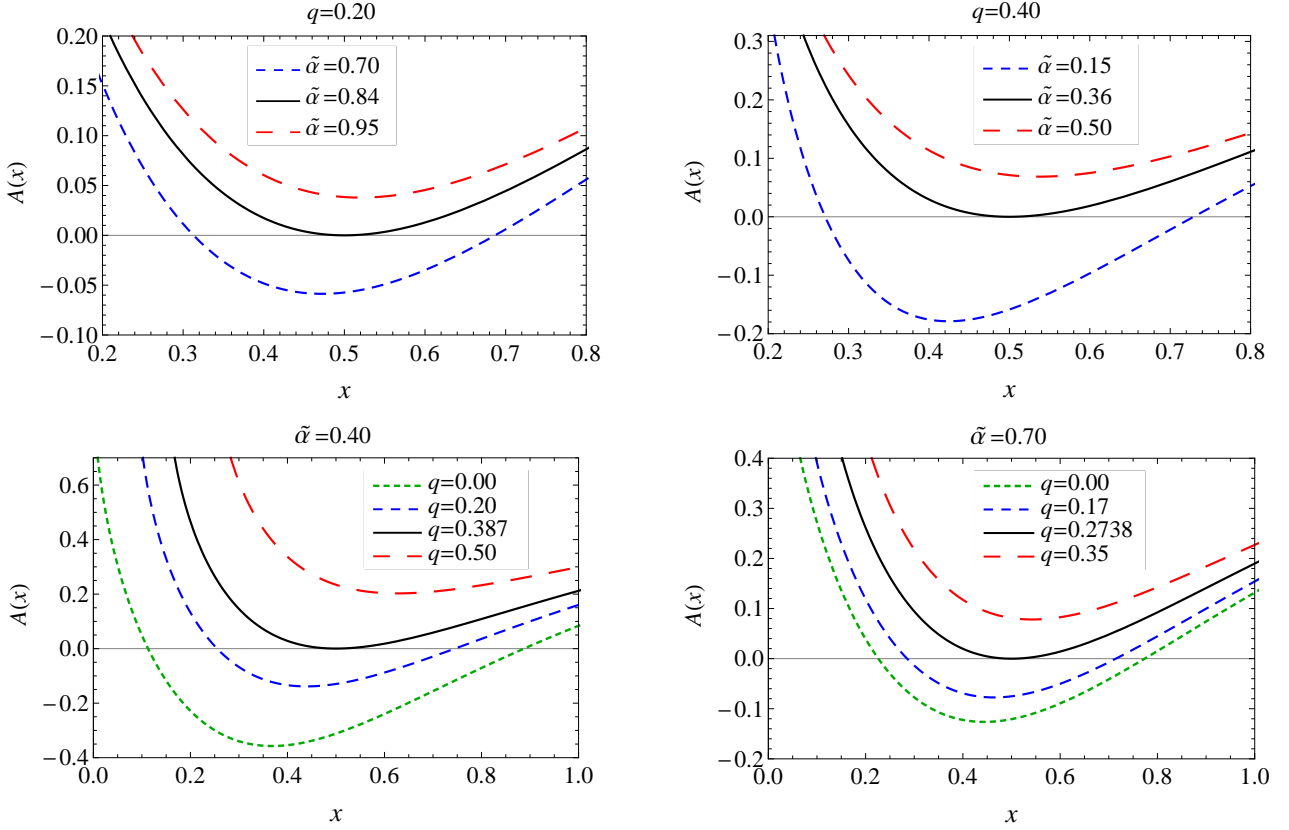


FIG. 1: (Upper panel) Plot showing the horizons for various values of GB coupling parameter $\tilde{\alpha}$ and fixed values of q . (Lower panel) Plot showing the horizons for different values of q and fixed $\tilde{\alpha}$. The black solid lines correspond to the extremal black holes.

the strong gravitational lensing, we adimensionlise the Charged black hole metric of EGB gravity (5) in terms of Schwarzschild radius $2M$ by defining $x = r/2M$, $T = t/2M$, $\tilde{\alpha} = \alpha/M^2$, and $q = Q/2M$. Then we have

$$d\tilde{s}^2 = (2M)^{-2}ds^2 = -A(x)dT^2 + \frac{1}{A(x)}dx^2 + C(x)(d\theta^2 + \sin^2\theta d\phi^2), \quad (8)$$

where

$$A(x) = 1 + \frac{2x^2}{\tilde{\alpha}} \left(1 \pm \sqrt{1 + \tilde{\alpha} \left(\frac{1}{x^3} - \frac{q^2}{x^4} \right)} \right), \quad C(x) = x^2. \quad (9)$$

It is clear that metric (8) possess a coordinate singularity at

$$A(x) = 0 \Rightarrow 4\tilde{\alpha}x^2 - 4\tilde{\alpha}x + \tilde{\alpha}(\tilde{\alpha} + 4q^2) = 0, \quad (10)$$

which admits two real positive roots given by

$$x_{\pm} = \frac{1}{2} \left(1 \pm \sqrt{1 - 4q^2 - \tilde{\alpha}} \right), \quad (11)$$

The two roots x_{\pm} correspond to the radii of black hole event horizon (x_+) and Cauchy horizon (x_-). It is clear

from Eq. (11) that for the existence of black hole, the allowed values for $\tilde{\alpha}$ are given by

$$\tilde{\alpha} \leq 1 - 4q^2 \text{ for } 0 \leq q \leq 0.5. \quad (12)$$

For a given value of q , there always exists an extremal value of $\tilde{\alpha} = \tilde{\alpha}_e = 1 - q^2$, for which black hole possess degenerate horizons i.e., $x_- = x_+ = x_e$, such that $\tilde{\alpha} < \tilde{\alpha}_e$ leads to two distinct horizons and $\tilde{\alpha} > \tilde{\alpha}_e$ leads to no-horizons (cf. Fig. 1). Similarly, one can find the extremal value of $q_e = \sqrt{1 - \tilde{\alpha}}/2$, for a given value of $\tilde{\alpha}$. The behavior of horizon radii with GB coupling parameter $\tilde{\alpha}$ and black hole charge q is shown in Fig. 2. Event horizon radius decreases whereas Cauchy horizon radius increases with increasing q or $\tilde{\alpha}$, such that Charged black holes of 4D EGB gravity always possess smaller event horizon as compared to Schwarzschild and Reissner-Nordstrom black holes.

III. LIGHT DEFLECTION ANGLE

In this section, we investigate the strong gravitational lensing in the Charged black holes of 4D EGB gravity to compute the deflection angles, location of relativistic

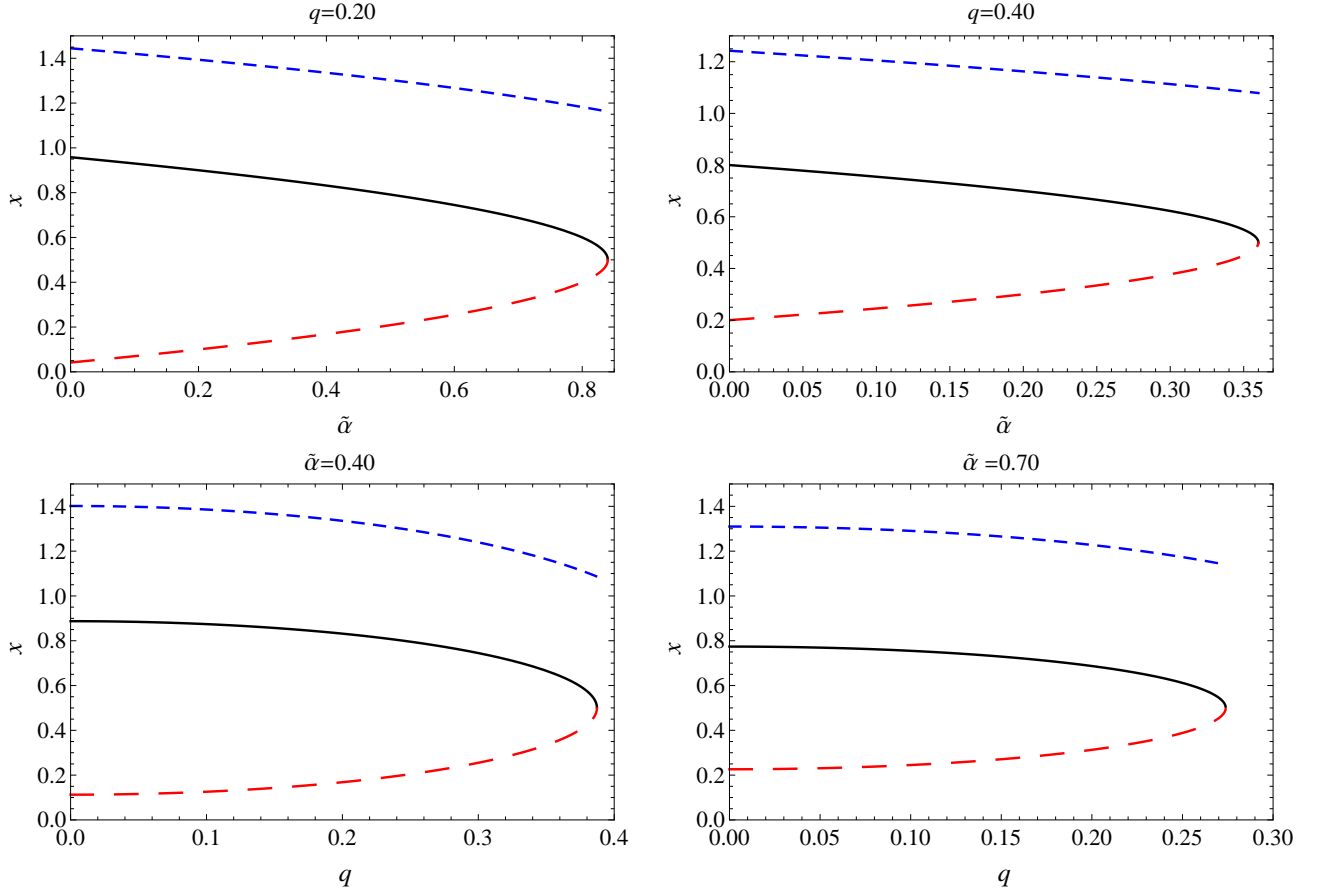


FIG. 2: The behavior of event horizon radii x_+ (solid black line), Cauchy horizon radii x_- (dashed red line), and photon sphere radii x_m (dashed blue line) with $\tilde{\alpha}$ and q .

images, their magnifications and the effect of $\tilde{\alpha}$ and q on them. We consider that light source S and observer O are sufficiently far from the black hole L , which acts as a lens, and they are nearly aligned. The light ray emanating from the source travel in straight path towards the black and only when it encounters the black hole gravitational field it suffers from the deflection (cf. Fig. 3). The amount of deflection suffered by light depends on the impact parameter u and distance of minimum approach x_0 , at which light suffer reflection and starts outward journey toward the observer [56]. Consider the propagation of light on the equatorial plane ($\theta = \pi/2$), as due to spherical symmetry, the whole trajectory of the photon is limited on the same plane. The projection of photon four-momentum along the Killing vectors of isotmetries are conserved quantities, namely the energy $\mathcal{E} = -p_\mu \xi_{(t)}^\mu$ and angular momentum $\mathcal{L} = p_\mu \xi_{(\phi)}^\mu$ are constant along the geodesics, where $\xi_{(t)}^\mu$ and $\xi_{(\phi)}^\mu$ are, respectively, the Killing vectors due to time-translational and rotational invariance [57].

Photons follow the null geodesics of metric (8), $d\tilde{s}^2 =$

0, which yields

$$\left(\frac{dx}{d\tau}\right)^2 \equiv \dot{x}^2 = \mathcal{E}^2 - \frac{\mathcal{L}^2 A(x)}{C(x)}, \quad (13)$$

where τ is the affine parameter along the geodesics. Photons traversing close to the black hole, experience radial turning points $\dot{x} = 0$ and follows the unstable circular orbits, whose radii x_m can be obtained from

$$\frac{A'(x)}{A(x)} = \frac{C'(x)}{C(x)}, \quad (14)$$

where prime corresponds to the derivative with respect to the x and the above admits at least one positive solution and then the largest real root is defined as the radius of the unstable circular photon orbits (cf. Fig. 2). A small radial perturbations drive these photons into the black hole or toward spatial infinity [57]. Due to spherical symmetry, these orbits generate a photon sphere around the black hole. The radii of photon orbits for Charged black holes of 4D EGB gravity decrease with increasing q and $\tilde{\alpha}$ (cf. Fig. 2).

Further, at the distance of minimum approach, we have

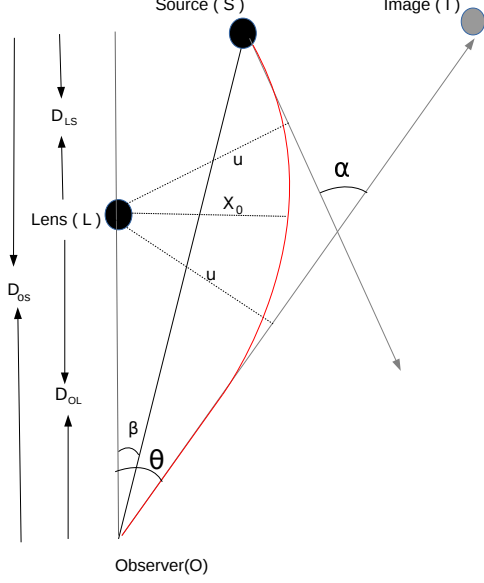


FIG. 3: Schematic for geometrical configuration of gravitational lensing.

[56]

$$\frac{dx}{d\phi} = 0, \Rightarrow u \equiv \frac{\mathcal{L}}{\mathcal{E}} = \sqrt{\frac{C(x_0)}{A(x_0)}}. \quad (15)$$

Following the method developed by Bozza [13], the total deflection angle suffered by the light in its journey from source to observer is given by

$$\alpha_D(x_0) = I(x_0) - \pi, \quad (16)$$

where

$$I(x_0) = 2 \int_{x_0}^{\infty} \frac{d\phi}{dx} dx = \int_{x_0}^{\infty} \frac{2 dx}{\sqrt{A(x)C(x)} \sqrt{\frac{C(x)A(x_0)}{C(x_0)A(x)} - 1}}, \quad (17)$$

The deflection angle increases as distance of minimum approach x_0 decreases and shows divergence as it approaches the photon sphere x_m [13]. In the strong deflection limit, we can expand the deflection angle near the photon sphere, for the purpose we define a new variable z as [13]

$$z = \frac{A(x) - A(x_0)}{1 - A(x_0)}, \quad (18)$$

the integral (16) can be re-written as

$$I(x_0) = \int_0^1 R(z, x_0) f(z, x_0) dz, \quad (19)$$

with the functions

$$R(z, x_0) = \frac{2\sqrt{C(x_0)(1 - A(x_0))}}{C(x)A'(x)}, \quad (20)$$

$$f(z, x_0) = \frac{1}{\sqrt{A(x_0) - \frac{A(x)}{C(x)}C(x_0)}}, \quad (21)$$

where $x = A^{-1}[(1 - A(x_0))z + A(x_0)]$. Making a Taylor series expansion of the function in Eq. (21), we get

$$f_0(z, x_0) = \frac{1}{\sqrt{\phi(x_0)z + \gamma(x_0)z^2}} \quad (22)$$

where

$$\phi(x_0) = \frac{1 - A(x_0)}{A'(x_0)C(x_0)} [C'(x_0)A(x_0) - A'(x_0)C(x_0)], \quad (23)$$

$$\begin{aligned} \gamma(x_0) = & \frac{(1 - A(x_0))^2}{2A'(x_0)^3C(x_0)^2} \left[2C(x_0)C'(x_0)A'(x_0)^2 \right. \\ & + A(x_0)A'(x_0)C(x_0)C''(x_0) - C(x_0)C'(x_0) \\ & \left. A(x_0)A''(x_0) - 2C'(x_0)^2A(x_0)A'(x_0) \right]. \end{aligned} \quad (24)$$

$R(z, x_0)$ is regular for all values of z , however, for $x_0 = x_m$, we have $\phi(x_0) = 0$ and $f_0 \approx 1/z$, which diverge as $z \rightarrow 0$. Following the above definitions, the diverging part in the integral Eq. (19) can be identified as [13]

$$I_D(x_0) = \int_0^1 R(0, x_m) f_0(z, x_0) dz, \quad (25)$$

whereas the regular part $I_R(x_0)$ is

$$\begin{aligned} I_R(x_0) = I(x_0) - I_D(x_0) = & \int_0^1 \left(R(z, x_0) f(z, x_0) \right. \\ & \left. - R(0, x_m) f_0(z, x_0) \right) dz. \end{aligned} \quad (26)$$

such that $I_D(x_0)$ has logarithmic divergence and $I_R(x_0)$ is regular with divergence subtracted from the complete integral (19). The deflection angle can be written in terms of x_0 as [13]

$$\alpha_D(x_0) = -a \log \left(\frac{x_0}{x_m} - 1 \right) + b + O(x_0 - x_m), \quad (27)$$

where

$$a = \frac{R(0, x_m)}{\sqrt{\gamma(x_m)}}, \quad (28)$$

$$b = -\pi + I_R(x_m) + a \log \left(\frac{2(1 - A(x_m))}{A'(x_m) \cdot x_m} \right), \quad (29)$$

The Eq. (27) is coordinate dependent, however, it can be written in terms of coordinate independent variable, impact parameter u , as follows

$$\alpha_D(u) = -\bar{a} \log \left(\frac{u}{u_m} - 1 \right) + \bar{b} + O(u - u_m), \quad (30)$$

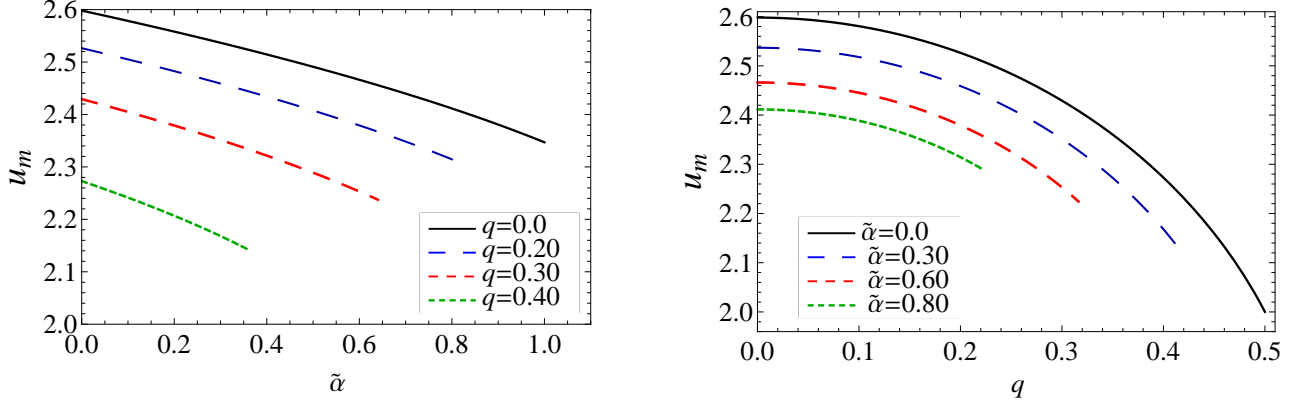


FIG. 4: Plot showing the impact parameter u_m for photon circular orbits with q and $\tilde{\alpha}$.

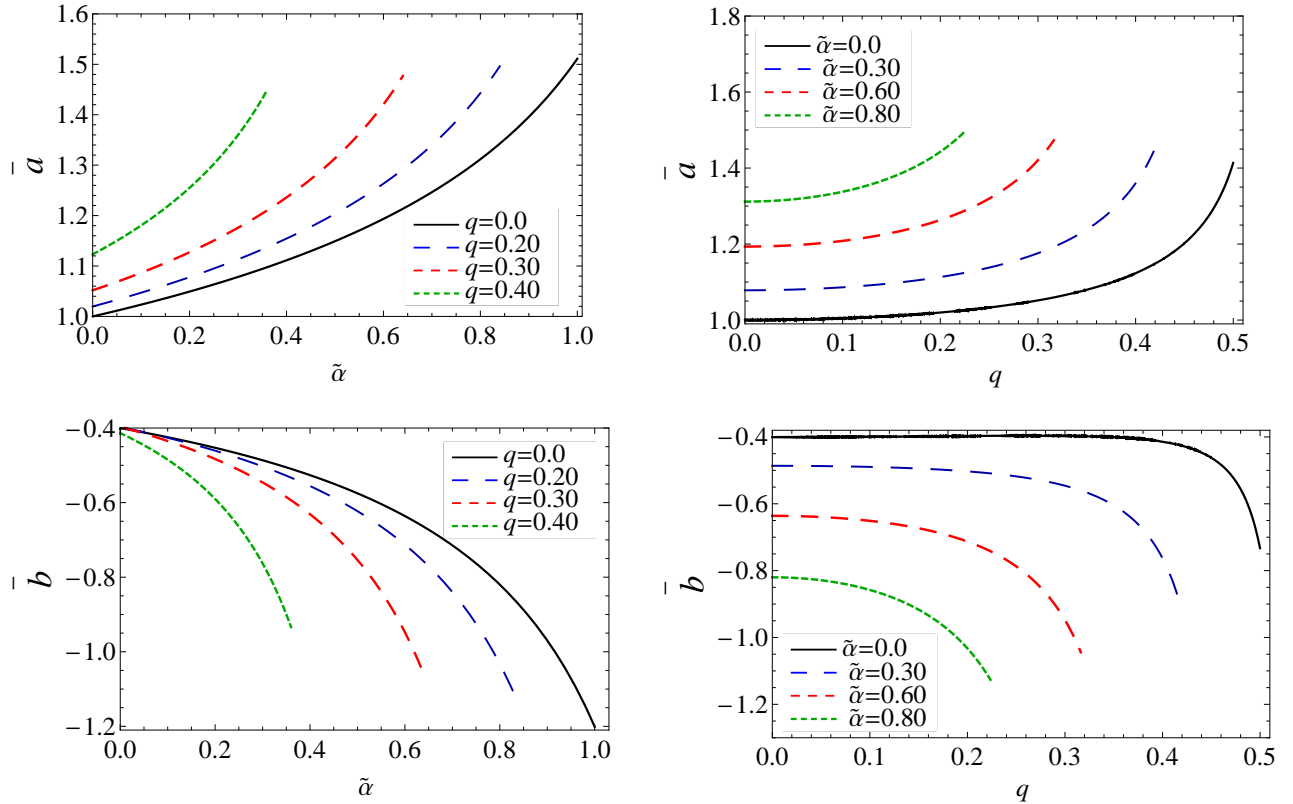


FIG. 5: Plot showing the behavior of strong lensing coefficients \bar{a} and \bar{b} as a functions of $\tilde{\alpha}$ (Left Panel) and q (Right Panel)

where

$$\bar{a} = \frac{a}{2}, \quad \bar{b} = -\pi + I_R(x_m) + \bar{a} \log \left(\frac{2\gamma(x_m)}{A(x_m)} \right), \quad (31)$$

where \bar{a} and \bar{b} are called the strong deflection limit coefficients. In Fig. 4, we plotted the impact parameter u_m for the photons moving on the unstable circular orbits around black hole as a functions of charge parameter q and GB coupling parameter $\tilde{\alpha}$. It is clear that u_m decrease with q and $\tilde{\alpha}$. The behavior of lensing

coefficients are shown in Fig. 5, which in the limits of $\tilde{\alpha} \rightarrow 0$ and $q = 0$, smoothly retain the values for the Schwarzschild black hole, viz., $\bar{a} = 1$ and $\bar{b} = -0.4002$ [12, 13]. Coefficient \bar{a} increases whereas \bar{b} decreases with increasing q or α . The resulting deflection angle $\alpha_D(u)$ is shown as a function of impact parameter u for various values of q and $\tilde{\alpha}$ in Fig. 6. For a fixed value of u , deflection angle decreases with increasing q or $\tilde{\alpha}$, therefore, the deflection angle is higher for Schwarzschild and Reissner-Nordstrom black holes than those for the

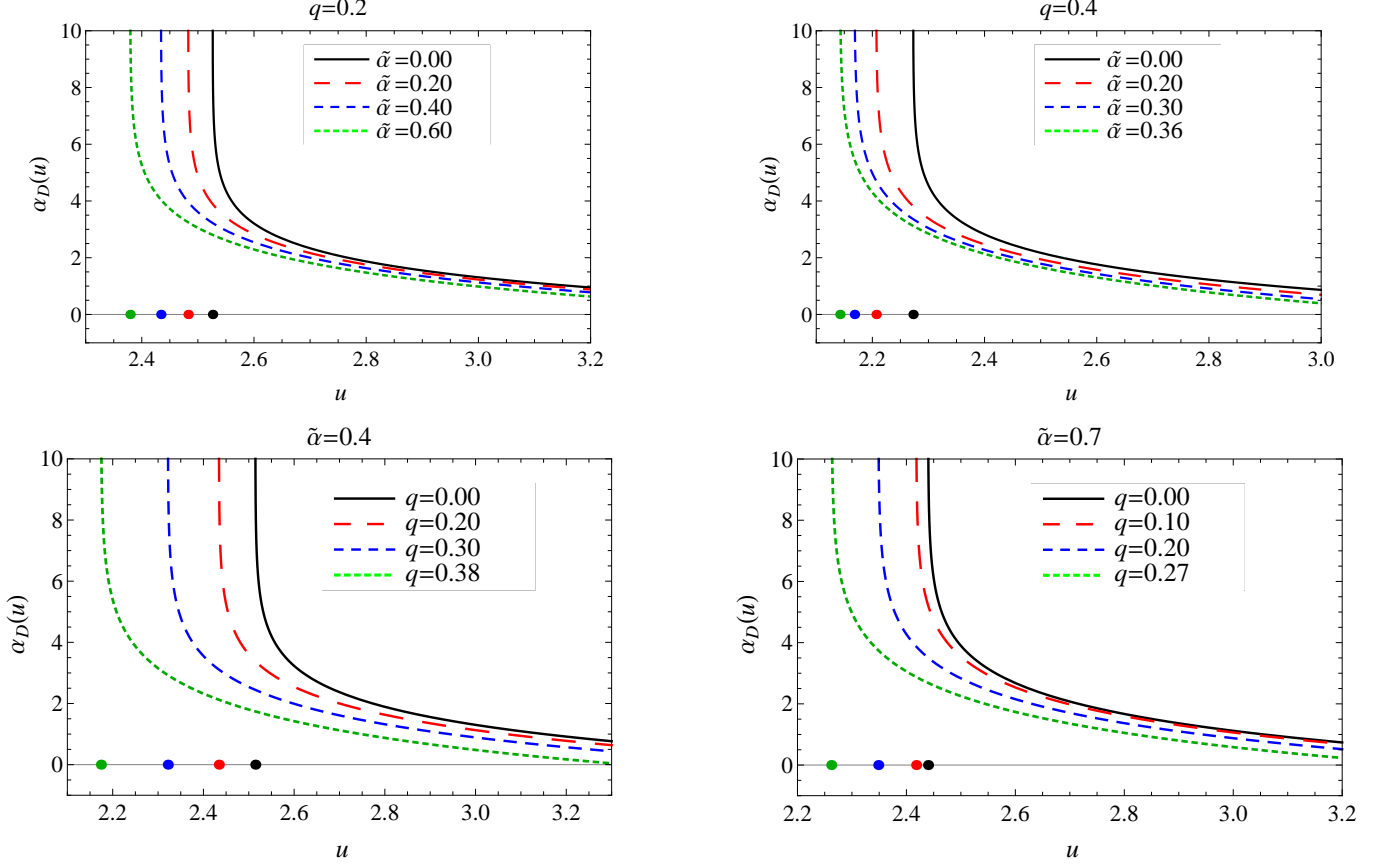


FIG. 6: Plot showing the variation of deflection as a functions impact parameter u for different values of $\tilde{\alpha}$ and q . The points on the horizontal axis correspond to the impact parameter $u = u_m$ at which deflection angle diverges.

Charged black holes of 4D EGB gravity. Figure 6 infers that the $\alpha_D(u)$ increases as impact parameter u approaches the u_m and becomes unboundedly large for $u = u_m$.

IV. STRONG LENSING OBSERVABLES

The deflection angle obtained in Eq. (30) is directly related to the positions and magnification of the relativistic images, which is given by lens equation [12]

$$\tan \beta = \tan \theta - \frac{D_{LS}}{D_{OS}} [\tan \theta + \tan(\alpha_D - \theta)], \quad (32)$$

where θ and β , respectively, are the angular separations of image and source from the black hole as shown in Fig. (3). The D_{LS} is the distance between the source and black hole and D_{OS} is distance from the source to the observer; all distances are expressed in terms of the Schwarzschild radius $x_s = R_s/2M$. For nearly perfect alignment of source, black hole and observer, viz. small values of θ and β , Eq. (32) reduces to the following form

[12]

$$\beta = \theta - \frac{D_{LS}}{D_{OS}} \Delta \alpha_n. \quad (33)$$

In case of strong lensing, photons complete multiple circular orbits around black hole before escaping toward observer, therefore α_D can be replaced by $2n\pi + \Delta \alpha_n$ in Eq. (32), with $n \in \mathbb{N}$ and $0 < \Delta \alpha_n \ll 1$.

The angular separation between the lens and n th relativistic images can be written as

$$\theta_n \simeq \theta_n^0 + \Delta \theta_n, \quad (34)$$

where

$$\begin{aligned} \theta_n^0 &= \frac{u_m}{D_{OL}} (1 + e_n), \\ \Delta \theta_n &= \frac{D_{OS}}{D_{LS}} \frac{u_m e_n}{D_{OL} \tilde{a}} (\beta - \theta_n^0), \\ e_n &= e^{\tilde{b} - 2n\pi/\tilde{a}}, \end{aligned} \quad (35)$$

where θ_n^0 corresponds to the angular separation when photon winds completely $2n\pi$ around the black hole and $\Delta \theta_n$ corresponds to the part exceeding $2n\pi$. Similarly,

magnification of images is another good source of information, which is defined as the ratio between the solid angles subtended by the image and the source, and for small angles it is given by [13]

$$\mu_n = \left(\frac{\beta}{\theta} \frac{d\beta}{d\theta} \bigg|_{\theta_n^0} \right)^{-1}. \quad (36)$$

Using Eqs. (33) and (35), the magnification (36) becomes:

$$\mu_n = \frac{1}{\beta} \left(\theta_n^0 + \frac{D_{OS}}{D_{LS}} \frac{u_m e_n}{D_{OL} \bar{a}} (\beta - \theta_n^0) \right) \left(\frac{D_{OS}}{D_{LS}} \frac{u_m e_n}{D_{OL} \bar{a}} \right), \quad (37)$$

which can be simplified further by making Taylor series expansion, thus the magnification of n th image on both the sides is given by [13]

$$\mu_n = \frac{1}{\beta} \left[\frac{u_m}{D_{OL}} (1 + e_n) \left(\frac{D_{OS}}{D_{LS}} \frac{u_m e_n}{D_{OL} \bar{a}} \right) \right]. \quad (38)$$

Thus magnification decreases exponentially with winding number n and the higher-order images become fainter. In order to relate the results obtained analytically with observations, Bozza defined the following observables [13]

$$\theta_\infty = \frac{u_m}{D_{OL}}, \quad (39)$$

$$s = \theta_1 - \theta_\infty, \quad (40)$$

$$r_{\text{mag}} = \frac{\mu_1}{\sum_{n=2}^{\infty} \mu_n}. \quad (41)$$

Since the outermost relativistic image is the brightest, the quantity s is the angular separation between the outermost image from the remaining bunch of relativistic images, r_{mag} is the ratio of the received flux between the first image and all the others images clustered at θ_∞ . For a nearly perfect alignment of source, black hole and observer, these observables can be simplified to [13]

$$s = \theta_\infty (e^{\frac{\bar{b}-2\pi}{\bar{a}}}), \quad (42)$$

$$r = e^{\frac{2\pi}{\bar{a}}}. \quad (43)$$

Once these strong lensing observables are known from observations, one can estimate the strong lensing coefficients \bar{a} and \bar{b} and compare with the theoretically calculated values.

V. LENSING BY GALACTIC SUPERMASSIVE BLACK HOLE

For numerical estimation, we consider a realistic case of a supermassive black hole Sgr A* at the center of our galaxy. Taking the distance to black hole $D_{OL} = 7.97 \times 10^3$ pc and mass of the black hole to be $3.98 \times 10^6 M_\odot$ [58],

we have tabulated the observables for Sgr A* in Table (I). We compared the results with those for the Schwarzschild ($\tilde{\alpha} = 0, q = 0$) and Reissner-Nordstrom black holes ($\tilde{\alpha} = 0$). It is worth to notice that, for Charged black holes of 4D EGB gravity, the angular separation between images are higher whereas their magnification are lower than those for the Schwarzschild and Reissner-Nordstrom black holes.

For a given value of D_{OL} , the limiting value of angular position is smaller than Schwarzschild case and decreases with q or $\tilde{\alpha}$. On the other hand the separation between the images s , for the Charged black holes of 4D EGB gravity is larger than the Schwarzschild black hole and it goes on increasing with increasing q or $\tilde{\alpha}$. So images are far away from the black hole and thereby less packed than in the Schwarzschild case. The observables are plotted against $\tilde{\alpha}$ and q in Fig.(7).

VI. CONCLUSION

The regularized 4D EGB gravity proposed in [31–33] is characterized by the non-trivial contribution of the GB quadratic term to the gravitational dynamics in 4D spacetime. Thereby, this 4D EGB gravity with quadratic-curvatures bypasses the Lovelock's theorem and yields the diffeomorphism invariance and second order equations of motion. The 4D EGB gravity possesses only the degrees of freedom of a massless graviton and thus free from the instabilities. Further, static and spherically symmetric black hole solutions of this 4D EGB gravity are also valid in other theories of gravity [34, 35, 37, 51].

With this motivation, we have analysed the strong gravitational lensing of light due to static spherically symmetric Charged black holes to 4D EGB gravity which besides the mass M , depends also on two parameters q and $\tilde{\alpha}$. We have examined the effects of q and $\tilde{\alpha}$, in a strong-field observation, to the lensing observables due to Charged black holes to 4D EGB gravity and compared with those due to Schwarzschild and Reissner-Nordstrom black holes of GR. We have numerically calculated the strong lensing coefficients \bar{a} and \bar{b} , and lensing observables θ_∞ , s , r_{mag} , u_m as functions of $\tilde{\alpha}$ and q for relativistic images. In turn, we have applied our results to the supermassive black hole Sgr A* at the center of our galaxy. Interestingly, we find that, \bar{a} increases when we increase q and $\tilde{\alpha}$ whereas \bar{b} and deflection angle α_D decrease, and observe the diverging behavior of deflection angle α_D when $u \rightarrow u_m$. In addition, for a fixed value of impact parameter, Charged black holes to 4D EGB gravity cause smaller deflection angle as compared to their GR counterparts.

We have also estimated some properties of relativistic images, the variations of θ_∞ , s , and r_{mag} , as function of $\tilde{\alpha}$ and q which are depicted in the Figs. 7. We have shown that the angular position of outermost relativistic images θ_∞ and relative magnification of images r_{mag} are

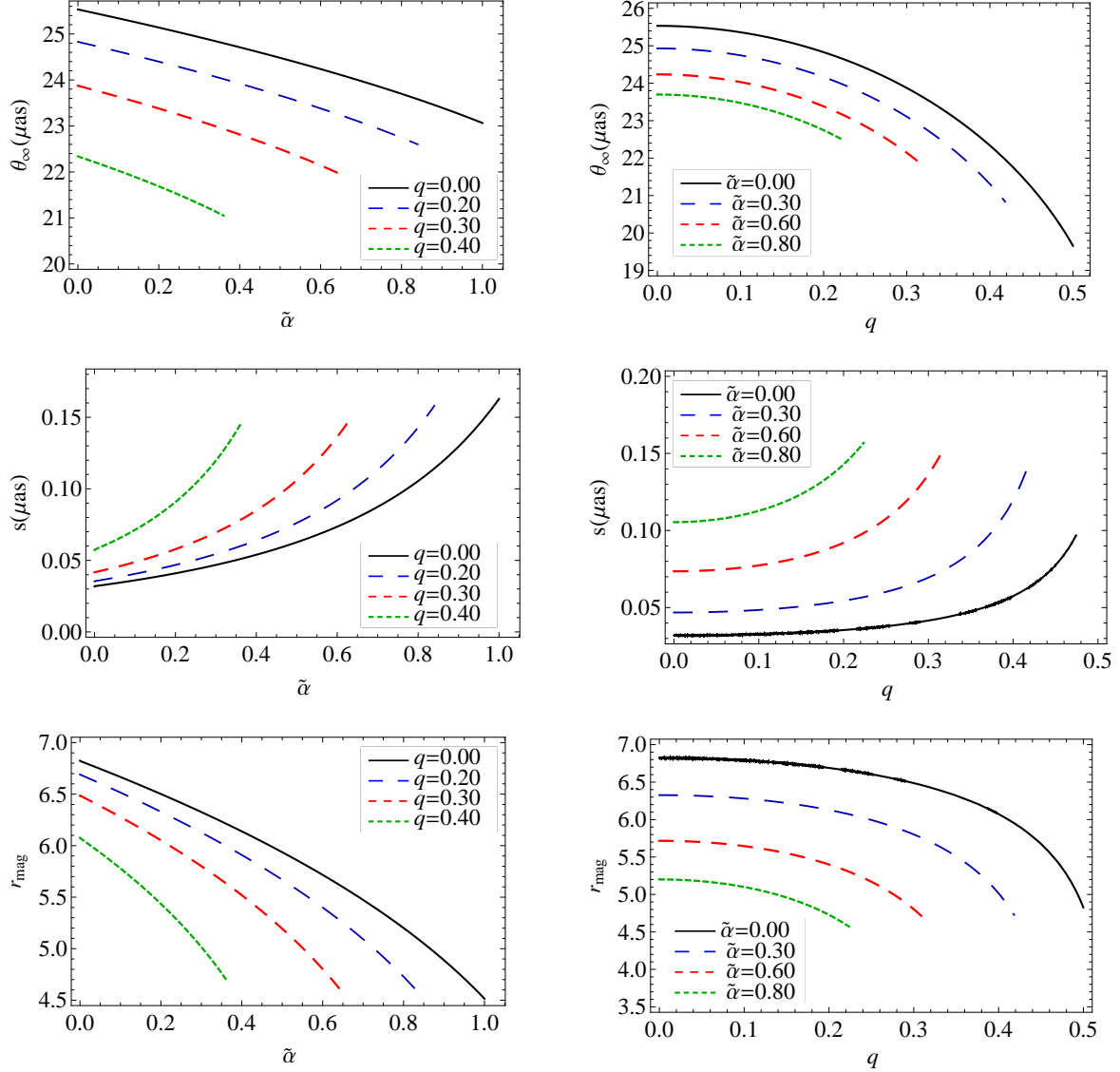


FIG. 7: Plots showing the behavior of strong lensing observables θ_∞ , s , and r_{mag} as a function $\tilde{\alpha}$ (Left panel) and q (Right panel) for Sgr A* black hole.

Observables	Schwarzschild	$\tilde{\alpha} = 0.4$				$\tilde{\alpha} = 0.7$			
		$q = 0.0$	$q = 0.2$	$q = 0.3$	$q = 0.38$	$q = 0.0$	$q = 0.1$	$q = 0.2$	$q = 0.27$
θ_∞ (μas)	25.530	24.710	23.920	22.814	21.365	23.976	23.762	23.077	22.234
s (μas)	0.0319	0.0539	0.0639	0.0848	0.1363	0.0873	0.0926	0.1132	0.1506
r_{mag}	6.820	6.138	5.909	5.519	4.805	5.473	5.389	5.092	4.637
u_m/R_s	2.597	2.514	2.434	2.321	2.174	2.439	2.417	2.348	2.262
\tilde{a}	1.000	1.111	1.154	1.236	1.419	1.246	1.265	1.339	1.471
\tilde{b}	-0.4004	-0.5263	-0.555	-0.6310	-0.8926	-0.7145	-0.7380	-0.8395	-1.0638

TABLE I: Estimates for lensing observables and strong lensing coefficients for the black hole Sgr A* for different values of q . $R_s = 2GM/c^2$ is the Schwarzschild radius.

decreasing function of both q and $\tilde{\alpha}$, but they decrease more sharply with q (cf. Fig. 7), while angular separation between images s increases with both q and $\tilde{\alpha}$. To conclude, we find that Charged black holes to 4D EGB gravity cause higher angular separation between images

but lower magnification than those for the Schwarzschild and Reissner-Nordstrom black holes.

The results presented here are the generalization of previous discussions, on the black holes in GR viz. Schwarzschild and Reissner-Nordstrom black holes

and black holes to 4D EGB gravity, and they are encompassed, respectively in the limits, $\alpha, q \rightarrow 0$, $\alpha \rightarrow 0$, and $q \rightarrow 0$.

Acknowledgments

S.G.G. would like to thank DST INDO-SA bilateral project DST/INT/South Africa/P-

06/2016, SERB-DST for the ASEAN project IMRC/AISTDF/CRD/2018/000042 and also IUCAA, Pune for the hospitality while this work was being done. R.K. would like to thank UGC for providing SRF. S.U.I would like to thank SERB-DST for the ASEAN project IMRC/AISTDF/CRD/2018/000042.

-
- [1] S. Doeleman *et al.*, Nature **455**, 78 (2008).
 - [2] K. Akiyama *et al.*, Astrophys. J. **875**, L1 (2019); K. Akiyama *et al.*, Astrophys. J. **875**, L4 (2019); K. Akiyama *et al.*, Astrophys. J. **875**, L5 (2019).
 - [3] B. Carter, Phys. Rev. D **174**, 1559 (1968).
 - [4] S. E. Gralla and A. Lupsasca, Phys. Rev. D **101**, 044031 (2020).
 - [5] A. Einstein, Science **84**, 506 (1936).
 - [6] J. L. Synge, Mon. Not. R. Astron. Soc. **131**, 463 (1966).
 - [7] C. Darwin, Proc. R. Soc. A **249**, 180 (1959).
 - [8] S. Liebes, Phys. Rev. **133**, B835 (1964); S. Refsdal, Mon. Not. Roy. Astron. Soc. **128**, 295 (1964); R. R. Bourassa and R. Kantowski, Astrophys. J. **195**, 13 (1975).
 - [9] P. Schneider, J. Ehlers, and E. E. Falco, *Gravitational Lenses* (Springer-Verlag, Berlin (1992)).
 - [10] K. S. Virbhadra and G. F. R. Ellis, Phys. Rev. D **62**, 084003 (2000).
 - [11] S. Frittelli, T. P. Kling and E. T. Newman, Phys. Rev. D **61**, 064021 (2000).
 - [12] V. Bozza, S. Capozziello, G. Iovane and G. Scarpetta, Gen. Rel. Grav. **33**, 1535 (2001).
 - [13] V. Bozza, Phys. Rev. D **66**, 103001 (2002).
 - [14] C. Will, *Theory and Experiment in Gravitational Physics* (Cambridge University Press, Cambridge (2018)).
 - [15] A. Bhadra, Phys. Rev. D **67**, 103009 (2003); R. Whisker, Phys. Rev. D **71**, 064004 (2005); E. F. Eiroa, Phys. Rev. D **71**, 083010 (2005), Braz. J. Phys. **35**, 1113 (2005); C. R. Keeton and A. O. Petters, Phys. Rev. D **72**, 104006 (2005); K. Sarkar and A. Bhadra, Class. Quant. Grav. **23**, 6101 (2006); C. R. Keeton and A. Petters, Phys. Rev. D **73**, 044024 (2006); S. V. Iyer and A. O. Petters, Gen. Rel. Grav. **39**, 1563 (2007); P. Zhang, M. Liguori, R. Bean and S. Dodelson, Phys. Rev. Lett. **99**, 141302 (2007); S. b. Chen and J. l. Jing, Phys. Rev. D **80**, 024036 (2009); R. Reyes, R. Mandelbaum, U. Seljak, T. Baldauf, J. E. Gunn, L. Lombriser and R. E. Smith, Nature **464**, 256 (2010).
 - [16] S. W. Wei, Y. X. Liu, C. E. Fu and K. Yang, JCAP **1210**, 053 (2012); G. Li, B. Cao, Z. Feng and X. Zu, Int. J. Theor. Phys. **54**, 3103 (2015); W. Javed, R. Babar and A. Övgün, Phys. Rev. D **99**, 084012 (2019); R. Shaikh, P. Banerjee, S. Paul and T. Sarkar, Phys. Rev. D **99**, 104040 (2019); S. Panpanich, S. Ponglertsakul and L. Tannukij, Phys. Rev. D **100**, 044031 (2019); K. Bronnikov and K. Baleevskikh, Grav. Cosmol. **25**, 44 (2019); R. Shaikh, P. Banerjee, S. Paul and T. Sarkar, Phys. Lett. B **789**, 270 (2019); C. Y. Wang, Y. F. Shen and Y. Xie, JCAP **1904**, 022 (2019); H. M. Reji and M. Patil, Phys. Rev. D **101**, 064051 (2020).
 - [17] V. Bozza and G. Scarpetta, Phys. Rev. D **76**, 083008 (2007); V. Bozza, Phys. Rev. D **78**, 103005 (2008), Int. J. Mod. Phys. D **26**, 1741013 (2017).
 - [18] K. S. Virbhadra and C. R. Keeton, Phys. Rev. D **77**, 124014 (2008).
 - [19] E. F. Eiroa and C. M. Sendra, Class. Quant. Grav. **28**, 085008 (2011).
 - [20] A. Övgün, Phys. Rev. D **99**, 104075 (2019).
 - [21] S. Panpanich, S. Ponglertsakul and L. Tannukij, Phys. Rev. D **100**, 044031 (2019).
 - [22] A. M. Nzioki, P. K. Dunsby, R. Goswami and S. Carloni, Phys. Rev. D **83**, 024030 (2011); M. L. Ruggiero [n], Gen. Rel. Grav. **41**, 1497-1509 (2009).
 - [23] J. Man and H. Cheng, JCAP **11**, 025 (2014); J. Sadeghi and H. Vaez, JCAP **06**, 028 (2014).
 - [24] C. Lanczos, Annals Math. **39** 842 (1938).
 - [25] D. Lovelock, J. Math. Phys. **12** 498 (1971).
 - [26] B. Zwiebach, Phys. Lett. **156B**, 315 (1985).
 - [27] S. Nojiri, S. D. Odintsov and V. K. Oikonomou, Phys. Rev. D **99**, 044050 (2019).
 - [28] T. Koivisto and D. F. Mota, Phys. Lett. B **644**, 104 (2007); L. Amendola, C. Charmousis and S. Davis, JCAP **0710**, 004 (2007).
 - [29] D.G. Boulware and S. Deser, Phys. Rev. Lett. **55**, 2656 (1985); D. L. Wiltshire, Phys. Lett. B **169**, 36 (1986); J. T. Wheeler, Nucl. Phys. B **268**, 737 (1986); R. G. Cai, Phys. Rev. D **65**, 084014 (2002); M. H. Dehghani, Phys. Rev. D **69**, 064024 (2004); S. G. Ghosh, M. Amir and S. D. Maharaj, Eur. Phys. J. C **77**, 530 (2017); S. G. Ghosh, Class. Quant. Grav. **35**, 085008 (2018).
 - [30] S. G. Ghosh, D. V. Singh and S. D. Maharaj, Phys. Rev. D **97**, 104050 (2018); S. Hyun and C. H. Nam, Eur. Phys. J. C **79**, 737 (2019); A. Kumar, D. Veer Singh and S. G. Ghosh, Eur. Phys. J. C **79**, 275 (2019); D. V. Singh, S. G. Ghosh and S. D. Maharaj, Annals Phys. **412**, 168025 (2020).
 - [31] D. Glavan and C. Lin, Phys. Rev. Lett. **124**, 081301 (2020).
 - [32] Y. Tomozawa, [arXiv:1107.1424 [gr-qc]].
 - [33] G. Cognola, R. Myrzakulov, L. Sebastiani and S. Zerbini, Phys. Rev. D **88**, 024006 (2013);
 - [34] R. G. Cai, L. M. Cao and N. Ohta, JHEP **1004**, 082 (2010); R. G. Cai, Phys. Lett. B **733**, 183 (2014).
 - [35] A. Casalino, A. Collea, M. Rinaldi and S. Vicentini, arXiv:2003.07068 [gr-qc].
 - [36] R. Konoplya and A. Zhidenko, Phys. Rev. D **101**, 084038 (2020).
 - [37] H. Lu and Y. Pang, arXiv:2003.11552 [gr-qc].
 - [38] R. A. Konoplya and A. F. Zinhailo, arXiv:2003.12492

- [gr-qc]; Y. P. Zhang, S. W. Wei and Y. X. Liu, arXiv:2003.10960 [gr-qc]; K. Hegde, A. N. Kumara, C. L. A. Rizwan, A. K. M. and M. S. Ali, arXiv:2003.08778 [gr-qc]; C. Y. Zhang, P. C. Li and M. Guo, arXiv:2003.13068 [hep-th]; M. S. Churilova, arXiv:2004.00513 [gr-qc];
- [39] P. G. S. Fernandes, arXiv:2003.05491 [gr-qc].
- [40] D. V. Singh, S. G. Ghosh and S. D. Maharaj, arXiv:2003.14136 [gr-qc].
- [41] S. G. Ghosh and S. D. Maharaj, arXiv:2003.09841 [gr-qc]; S. G. Ghosh and R. Kumar, arXiv:2003.12291 [gr-qc].
- [42] D. V. Singh and S. Siwach, arXiv:2003.11754 [gr-qc]; A. Kumar and R. Kumar, arXiv:2003.13104 [gr-qc]; A. Kumar, D. V. Singh and S. G. Ghosh, arXiv:2003.14016 [gr-qc]. A. Kumar and S. G. Ghosh, arXiv:2004.01131 [gr-qc].
- [43] S. W. Wei and Y. X. Liu, arXiv:2003.07769 [gr-qc]; R. Kumar and S. G. Ghosh, arXiv:2003.08927 [gr-qc].
- [44] S. U. Islam, R. Kumar and S. G. Ghosh, arXiv:2004.01038 [gr-qc]; X. H. Jin, Y. X. Gao and D. J. Liu, arXiv:2004.02261 [gr-qc]; M. Heydari-Fard and H. R. Sepangi, arXiv:2004.02140 [gr-qc].
- [45] M. Guo and P. C. Li, arXiv:2003.02523 [gr-qc].
- [46] R. A. Konoplya and A. F. Zinhailo, arXiv:2003.01188 [gr-qc].
- [47] P. G. Fernandes, P. Carrilho, T. Clifton and D. J. Mulryne, arXiv:2004.08362 [gr-qc].
- [48] K. Jusufi, A. Banerjee and S. G. Ghosh, arXiv:2004.10750 [gr-qc].
- [49] S. A. Hosseini Mansoori, arXiv:2003.13382 [gr-qc]; M. Cuyubamba, arXiv:2004.09025 [gr-qc].
- [50] W. Ai, [arXiv:2004.02858 [gr-qc]].
- [51] R. A. Hennigar, D. Kubiznak, R. B. Mann and C. Pollack, [arXiv:2004.09472 [gr-qc]].
- [52] F. Shu, [arXiv:2004.09339 [gr-qc]].
- [53] M. Gurses, T. C. Sisman and B. Tekin, [arXiv:2004.03390 [gr-qc]].
- [54] S. Mahapatra, arXiv:2004.09214 [gr-qc].
- [55] T. Kobayashi, arXiv:2003.12771 [gr-qc].
- [56] S. Weinberg, *Gravitation and Cosmology: Principles and Applications of the General Theory of Relativity* (New York: Wiley, 1972).
- [57] S. Chandrasekhar, *The Mathematical Theory of Black Holes* (Oxford University Press, New York, 1992).
- [58] T. Do *et al.*, *Science* **365**, 664 (2019).